Partition function zeros of the one-dimensional Blume-Capel model in transfer matrix formalism

R. G. Ghulghazaryan, K. G. Sargsyan, and N. S. Ananikian
Department of Theoretical Physics, Yerevan Physics Institute, Alikhanian Brothers 2, 375036, Yerevan, Armenia
(Received 28 December 2006; revised manuscript received 6 June 2007; published 2 August 2007)

Zeros of the partition function of the one-dimensional ferromagnetic and antiferromagnetic Blume-Capel models have been studied by using the transfer matrix method in the thermodynamic limit and for finite size chains. The equation for the distribution of zeros of the partition function in the thermodynamic limit is derived. The distribution of the Yang-Lee and Fisher zeros are studied for a variety of values of the parameters of the model. Densities of the Yang-Lee and Fisher zeros are investigated and a singular behavior of the corresponding densities of zeros at the edge points is shown. The edge singularity exponents are calculated analytically for the densities of the Yang-Lee and Fisher zeros. It is found that for both cases edge singularity exponents are universal and equal to $\sigma=-\frac{1}{2}$.

DOI: 10.1103/PhysRevE.76.021104 PACS number(s): 05.50.+q, 05.70.Fh, 75.40.Mg

I. INTRODUCTION

More than 50 years ago Yang and Lee proposed a method for studying phase transitions based on the study of the partition function zeros [1]. They considered the partition function of the Ising model as a polynomial in activity [$\exp(-2H/kT)$, where H is a magnetic field] and studied the distribution of zeros of the partition function in the complex activity plane (the Yang-Lee zeros). Moreover, they proved the famous circle theorem which states that zeros of the partition function of the ferromagnetic Ising model are distributed on a unit circle in the complex activity plane. Also, a direct connection between the function representing the density of the partition function zeros with the thermodynamic functions describing the phase transition was shown [1].

Later, Fisher [2] initiated a study of zeros of the partition function in the complex temperature plane (the Fisher zeros) and found an analytical solution for the Ising model in zero magnetic field on a square lattice.

Since that time many papers have been devoted to the application of theory of the partition function zeros for studying different statistical physical models on various lattices [3–6]. The circle theorem was discussed and proved for more general lattice systems and the examples of violation of the circle theorem were obtained [7]. Singular behavior for the density of the Yang-Lee zeros is obtained at the Yang-Lee edges [9]. Moreover, it was shown that the singularities of the thermodynamic quantities may be obtained using the density of the partition function zeros [10]. Also, different Griffiths-type inequalities are demonstrated on the basis of the Yang-Lee circle theorem [3,8]. Similar results were found for the Fisher zeros [11]. Usually the distribution of the Fisher zeros strongly depends on the model. Moreover, the Fisher zeros are more sensitive to the type of interactions, the dimensionality of the system, boundary conditions, and the type of the lattice than the Yang-Lee zeros for which universality properties have been proved. In general, the calculation of the Fisher zeros is a difficult analytical task and the main results for Fisher zeros were found numerically [11].

Nowadays the transfer-matrix method is a standard tool for studying the partition function zeros of the one and higher dimensional systems [3,12]. Much attention is devoted to the investigation of the one-dimensional and ladder models that may give us a key for understanding the behavior and properties of more complicated high dimensional models [12].

Although one-dimensional systems with finite range and classical interactions, i.e., interactions involving only commuting interacting variables, in the thermodynamic limit cannot display a phase transition at nonzero temperature, they can exhibit a critical behavior on the complex activity and temperature plains at the Yang-Lee and Fisher edges, respectively [6,13,14]. Using the transfer matrix method, the universal character of the Yang-Lee edge singularity for classical one-dimensional models with finite range interactions is proved [13,14]. The behavior of transfer matrix eigenvalues of one-dimensional models in real and complex magnetic fields is studied for the Yang-Lee zeros by Wang and Kim [14]. They showed that for a lattice system in a real magnetic field, the condition of phase transition requires that the largest eigenvalues of the transfer matrix be twofold degenerate. Also, in the gap close to the positive real semiaxis where the Yang-Lee zeros are absent (no phase transition), the eigenvalues of the transfer matrix must be real [14]. Thus at the Yang-Lee edge, the maximal by modulus eigenvalue must be twofold degenerate. The universal character of the Yang-Lee edge singularity for one-dimensional models has been confirmed by a number of studies of spin-1/2, -1, and -3/2 Ising, Blume-Capel, Blume-Emery-Griffith, N-vector, and other models [3,15,16]. Almeida and Dalmazi [17] studied the Yang-Lee zeros of the one-dimensional Blume-Capel ferromagnetic model with periodic boundary conditions on connected and nonconnected rings using the Feynman diagrams method. They studied the departure of the Yang-Lee zeros from the unit circle as the temperature increased beyond some limit and showed that in the thermodynamic limit the zeros of Blume-Capel models on the static (connected rings) and on the dynamical (Feynman diagrams) lattices tend to overlap. Recently, the Yang-Lee and Fisher zeros and the corresponding edge singularities have been investigated for the one-dimensional Q-state Potts model [6]. It has been shown that the Yang-Lee and Fisher edge singularity exponents for the one-dimensional Q-state Potts model are equal to each other and equal to $\sigma=-\frac{1}{2}$.

 ©2007 The American Physical Society

Although general theorems on the distribution of Yang-Lee zeros are known, and universal behavior is established for the Yang-Lee edge singularities, very poor general results are known for the Fisher zeros and the Fisher edge singularities.

In this paper the transfer matrix method is used to study the Yang-Lee and Fisher zeros of both the ferromagnetic and antiferromagnetic one-dimensional Blume-Capel models with periodic boundary conditions. Analytical equation for zeros of the partition function is derived and used for numerical calculation of the Yang-Lee and Fisher zeros. The densities of the partition function zeros are studied and edge singularity exponents are calculated. It is shown that edge singularity exponents for both the Yang-Lee and Fisher zeros coincide and are equal to $\sigma=-\frac{1}{2}$. Also, symbolic and numerical calculations on finite size chains were performed to compute the partition function zeros for up to $N=1024$ spins. The distributions of the Yang-Lee and Fisher zeros for finite size system are consistent with the corresponding distributions in the thermodynamic limit. The study of zeros of the partition function for finite systems with a large number of spins requires solutions of high order polynomial equations. These solutions may show numerical instabilities in the complex plane. Some details of the numerical procedure for finding zeros of finite size partition function for a large number of spins $N>10^3$ are discussed.

II. PARTITION FUNCTION AND ITS ZEROS

The Blume-Capel (BC) model [18] is a special case of the spin-1 Blume-Emery-Griffiths (BEG) model [19]. The BC model may describe a variety of interesting physical systems. In particular, it describes phase separation driven by superfluidity in ^{3}He-^{4}He mixtures [20], inverse melting transformations of the metallic alloys [21], liquid crystals [22], the liquid-liquid transition theory for polyamorphous materials [23], vortex lines in disordered high temperature superconductors [24], cold denaturation of proteins [25], and different types of polymeric systems [26]. The BC model has played an important role in the development of the theory of tricritical phenomena and has been actively studied over the years.

The Hamiltonian of the one-dimensional BC model [18] has the form

$$-\beta H = J\sum_{i=1}^{N} s_i s_{i+1} - \Delta\sum_{i=1}^{N} s_i^2 + h\sum_{i=1}^{N} s_i, \tag{1}$$

where $\beta=1/(k_BT)$ and $s_i=0,\pm 1$ is the spin variable at each site of the chain and N is the number of spins on the chain. The partition function of the system is defined as

$$Z_N = \sum_{\{s_i\}} e^{-\beta H}, \tag{2}$$

where the summation goes over all configurations of the system. For analytical calculations it is convenient to define the transfer matrix of the BC model in a symmetric form,

$$V(s_i,s_{i+1}) = \exp\left[Js_is_{i+1} - \tfrac{1}{2}\Delta(s_i^2+s_{i+1}^2) + \tfrac{1}{2}h(s_i+s_{i+1})\right],$$

and

$$V = \begin{pmatrix} e^{J-\Delta-h} & e^{-(\Delta+h)/2} & e^{-J-\Delta} \\ e^{-(\Delta+h)/2} & 1 & e^{-(\Delta-h)/2} \\ e^{-J-\Delta} & e^{-(\Delta-h)/2} & e^{J-\Delta+h} \end{pmatrix}. \tag{3}$$

Imposing periodic boundary conditions on the chain ($s_{N+1}=s_1$) the following expression for the partition function (2) may be derived:

$$Z_N = \mathrm{Tr}V^N = \lambda_1^N + \lambda_2^N + \lambda_3^N, \tag{4}$$

where λ_i $(i=1,2,3)$ are the eigenvalues of the transfer matrix (3) defined by the characteristic equation

$$\lambda^3 - (1+e^{J-\Delta}x)\lambda^2 + e^{-\Delta}[x(e^J-1)+e^{-\Delta}(e^{2J}-e^{-2J})]\lambda - e^{-2\Delta}(e^{2J}-1)(1-e^{-J})^2 = 0, \tag{5}$$

and $x=e^h+e^{-h}$.

In the thermodynamic limit $(N\to\infty)$, the contribution of the eigenvalue of highest modulus to the partition function is dominated, i.e., for $|\lambda_1|>|\lambda_i|$ $(i=2,3)$,

$$Z_N = \lambda_1^N\left[1+\left(\frac{\lambda_2}{\lambda_1}\right)^N + \left(\frac{\lambda_3}{\lambda_1}\right)^N\right] \simeq \lambda_1^N. \tag{6}$$

Thus the thermodynamic properties of the system in the region of the complex activity or temperature plane where one of the eigenvalues, say λ_1, has maximal modulus are defined by the corresponding eigenvalue λ_1. Now, suppose that in the corresponding complex plain there exists a region where another eigenvalue λ_2 is dominated. At the boundary between these two regions where different eigenvalues λ_1 and λ_2 dominate, thermodynamic functions possess a nonanalytical behavior and the boundary is defined by the condition [3]

$$|\lambda_1| = |\lambda_2| > |\lambda_3|. \tag{7}$$

In the thermodynamic limit the contribution of the smallest by modulus eigenvalue λ_3 into the partition function may be neglected and the partition function becomes

$$Z_N = \lambda_1^N\left(1+\left|\frac{\lambda_2}{\lambda_1}\right|^N e^{i\varphi N}\right) \simeq \lambda_1^N(1+e^{i\varphi N}), \tag{8}$$

where from condition (7) for λ_2 we substitute

$$\lambda_2 = \lambda_1 e^{i\varphi}. \tag{9}$$

Since $|\lambda_1|>0$ from Eq. (8) it follows that zeros of the partition function correspond to values of φ defined by the equation

$$1+e^{i\varphi N}=0, \tag{10}$$

from which

$$\varphi \equiv \varphi_p = \frac{(2p+1)\pi}{N}, \quad p=0,\ldots,N-1. \tag{11}$$

Based on Vieta's theorem, for the eigenvalues of the transfer matrix (3) we can write

$$\lambda_1+\lambda_2+\lambda_3 = a_2,$$

$$\lambda_1\lambda_2+\lambda_2\lambda_3+\lambda_3\lambda_1 = a_1, \tag{12}$$

$$\lambda_1\lambda_2\lambda_3 = a_0,$$

where

$$a_2 = 1 + e^{J-\Delta}x,$$

$$a_1 = e^{-\Delta}[x(e^J - 1) + e^{-\Delta}(e^{2J} - e^{-2J})],$$

$$a_0 = e^{-2\Delta}(e^{2J} - 1)(1 - e^{-J})^2.$$

Using Eqs. (9) and (12) analytical expressions for eigenvalues can be found,

$$\lambda_{1,2} = \frac{[a_1a_2 - (1 + 2\cos\varphi)^2 a_0]e^{\mp i(\varphi/2)}}{2\cos(\varphi/2)[a_2^2 - (1 + 2\cos\varphi)a_1]}, \tag{13}$$

$$\lambda_3 = a_2 - \frac{a_1a_2 - (1 + 2\cos\varphi)^2 a_0}{a_2^2 - (1 + 2\cos\varphi)a_1}. \tag{14}$$

On the other hand, using Eq. (9) and excluding λ's from Eq. (12), Eq. (15) for zeros of the partition function can be derived,

$$F(h,\Delta,J,\varphi) \equiv (1 + 2\cos\varphi)^3 a_0^2 + 4\cos^2\frac{\varphi}{2}(a_1^3 + a_0a_2^3) - a_1^2a_2^2 - 2(1 + 2\cos\varphi)(2 + \cos\varphi)a_0a_1a_2 = 0. \tag{15}$$

Note, that it is required that zeros of the partition function be solutions to Eq. (15) but not all solutions to Eq. (15) correspond to zeros of the partition function. Zeros of the partition function should also satisfy the condition (7), where eigenvalues are defined in Eqs. (13) and (14). Thus Eq. (15) and the condition (7) are the necessary and sufficient conditions for defining zeros of the partition function.

In the study above we did not consider the case when all eigenvalues have the same modulus and differ only by phases. This gives another possibility for zeros of the partition function to appear and may correspond to "pseudotricritical" behavior of the model. In this case, the partition function may be written in the form

$$Z_N = \lambda_1^N(1 + e^{\imath\varphi N} + e^{\imath\psi N}), \tag{16}$$

where $\lambda_2 = \lambda_1 e^{\imath\varphi}$ and $\lambda_3 = \lambda_1 e^{\imath\psi}$. Since $|\lambda_1| > 0$ the partition function becomes zero if

$$1 + e^{\imath\varphi N} + e^{\imath\psi N} = 0. \tag{17}$$

The solution to the system of trigonometric Eqs. (17) with respect to φ and ψ has the form

$$\varphi = \frac{2\pi}{3N}, \quad \psi = -\varphi + \frac{2\pi p}{N}, \quad p = 0, \ldots, N-1. \tag{18}$$

Using Eq. (18) we performed a number of numerical tests for a wide range of J and Δ values and did not find any zeros. Thus no pseudotricritical behavior is found for the one-dimensional Blume-Capel model and the partition function zeros are defined by Eq. (15) and condition (7) only.

III. DENSITY OF THE PARTITION FUNCTION ZEROS

The density of the partition function zeros may be found using Eqs. (11) and (15). The solution of Eq. (15) with respect to $\mu = e^h$ (the Yang-Lee zeros) or $z = e^J$ (the Fisher zeros) depends on the value of the parameter φ given in Eq. (11). In the thermodynamic limit, solutions to Eq. (15) define continuous multibranch mappings $\gamma_i(\varphi)$, where γ stands for μ or z for the Yang-Lee and Fisher zeros, respectively, and i is the index of the branch. Let us consider one of the branches of this mapping. According to Eq. (11) the number of the partition function zeros corresponding to the values of φ from the interval $[\varphi_{p_1}, \varphi_{p_2}]$ and located on the same branch is proportional to the difference $\varphi_{p_2} - \varphi_{p_1}$. The integers p_2, p_1 are defined by Eq. (11). The density of the partition function zeros between the points $\gamma_i(\varphi_{p_1})$, $\gamma_i(\varphi_{p_2})$ may be found as the ratio of the difference $\varphi_{p_2} - \varphi_{p_1}$ to the length of the curve $\gamma_i(\varphi)$. Thus for the density of the partition function zeros we get

$$\tilde{g}_i(\varphi_{p_1}, \varphi_{p_2}) \propto \frac{\varphi_{p_2} - \varphi_{p_1}}{\int_{\varphi_{p_1}}^{\varphi_{p_2}} \sqrt{(\partial \mathrm{Re}\,\gamma_i/\partial\varphi)^2 + (\partial \mathrm{Im}\,\gamma_i/\partial\varphi)^2}\, d\varphi}. \tag{19}$$

In the thermodynamic limit, assuming that the interval $\varphi_{p_2} - \varphi_{p_1}$ is small, one obtains

$$g_i(\varphi) \equiv \tilde{g}_i(\varphi, \varphi + d\varphi) \propto \frac{1}{\sqrt{(\partial \mathrm{Re}\ \gamma_i/\partial\varphi)^2 + (\partial \mathrm{Im}\ \gamma_i/\partial\varphi)^2}}. \tag{20}$$

Let us define the edge point as a point where the line of the partition function zeros end up. Let γ_e be an edge point and φ_e be the corresponding phase. After expanding the function $F(\gamma,\varphi) \equiv F(h,\Delta,J,\varphi)$ of Eq. (15) in Taylor series up to the second order terms in γ_e, φ_e and solving it with respect to γ, we can get the behavior of the $\gamma_i(\varphi)$ in the vicinity of the edge point γ_e. Using this procedure a singular behavior for density of the partition function zeros at the edge points is shown and the edge singularity exponent σ is calculated for the Yang-Lee and Fisher zeros as given in the next sections below.

IV. YANG-LEE ZEROS

The Yang-Lee zeros of the BC model may be obtained by solving the eighth order polynomial Eq. (15) with respect to $\mu = e^h$ and taking only zeros that satisfy condition (7). Some examples of the distribution of the ferromagnetic Yang-Lee zeros are given in Fig. 1. In Fig. 1 plots of the Yang-Lee zeros for the thermodynamic limit and finite size system calculations are shown. We see that the Yang-Lee zeros lie on a single or several curves that end up at some points called the Yang-Lee edges. From the plots one can see that the distribution of the Yang-Lee zeros of the thermodynamic limit ($N = 10\,000$) and finite size system ($N = 1024$) calculations are very similar and almost indistinguishable.

According to the transfer matrix formalism the Yang-Lee edges are defined by the condition that the eigenvalue with maximal modulus is twofold degenerated [3]. Thus from condition (9) at the Yang-Lee edges $\varphi = 0$. The Yang-Lee

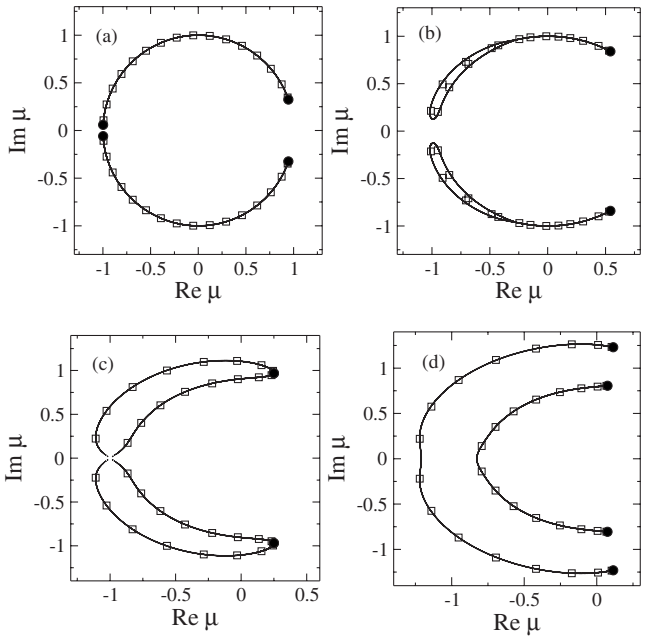

FIG. 1. The Yang-Lee zeros of the ferromagnetic one-dimensional Blume-Capel model on complex $\mu=e^{h}$ plane for $y=e^{\Delta}=3$ and different values of parameter $z=e^{J}$: (a) $z=4$, (b) $z=20/9$, (c) $z=2$, (d) $z=20/11$. Continuous lines correspond to the Yang-Lee zeros in the thermodynamic limit ($N=10\,000$). The Yang-Lee edge singularity points are marked with bold points. Boxes correspond to exact finite size system calculation data for $N=16$ spins. The data for finite size system calculation for $N=1024$ shown as dots is indistinguishable from the thermodynamic limit data.

edge points are shown in Fig. 1 as bold points. In order to study the behavior of the density of the Yang-Lee zeros in the vicinity of the Yang-Lee edge points ($\varphi=0$) consider the Taylor series expansion of Eq. (15) up to the second order terms in φ,

$$\mu_i(\varphi) \approx \mu_e + \frac{\partial^2 \mu_i}{\partial^2 \varphi}\varphi^2 + o(\varphi^4), \tag{21}$$

with zero linear term because $F(h,\Delta,J,\varphi)$ is an even function of φ. Thus from Eqs. (20) and (21) for the density of the Yang-Lee zeros at the Yang-Lee edges

$$g_{yl}(\varphi) \propto |\varphi|^{-1}. \tag{22}$$

The polar angle θ is introduced for the Yang-Lee zero μ. At the Yang-Lee edge, μ_e,θ_e corresponds to $\varphi=0$. Close to the Yang-Lee edge point the density of the Yang-Lee zeros may be written in the form $g(\theta)\propto|\theta-\theta_e|^{\sigma}$, where σ is the Yang-Lee edge singularity exponent. For calculating the critical exponent σ let us calculate the length of the curve between the points $\mu_i(\theta)$ and $\mu(\theta_e)$ over which the Yang-Lee zeros are distributed,

$$(\theta-\theta_e)R_i = \sqrt{\mathrm{Re}(\mu_i-\mu_e)^2 + \mathrm{Im}(\mu_i-\mu_e)^2}, \tag{23}$$

where R_i is the radius of curvature of ith branch of the Yang-Lee zeros distribution curve. From Eqs. (23) and (21) it follows that

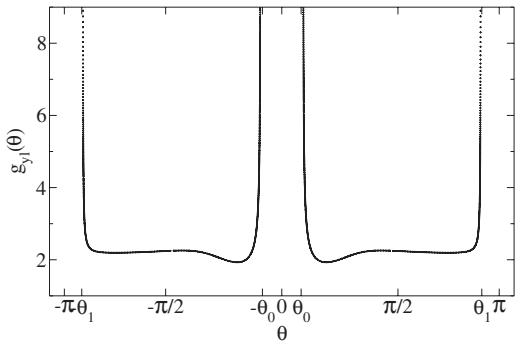

FIG. 2. Dependence of density of the Yang-Lee zeros on θ in the thermodynamic limit ($N=10\,000$) for $y=3$ and $z=4$. The density of zeros shows singular behavior at four Yang-Lee edges shown in Fig. 1(a) which are complex conjugate numbers with arguments $\pm\theta_0$ and $\pm\theta_1$. Here the data along the y axes is given in arbitrary units and $\theta_0=0.334$ and $\theta_1=3.08$.

$$\varphi^2 \propto (\theta-\theta_0). \tag{24}$$

Using Eqs. (22) and (24) we get

$$g_{yl}(\theta) \propto |\theta-\theta_e|^{-1/2}, \tag{25}$$

and $\sigma=-\frac{1}{2}$. Note that in our treatment the branch for which the edge singularity exponent σ is calculated was chosen randomly. Thus for all the branches of the Yang-Lee zeros distribution curves the Yang-Lee edge singularity exponent is universal and equal to $\sigma=-\frac{1}{2}$. This result is in good agreement with the previous studies of the Yang-Lee edge singularities [3,13,14]. The plot of the density of the Yang-Lee zeros in the thermodynamic limit is given in Fig. 2 where a singular behavior of the density $g_{yl}(\theta)$ at the Yang-Lee edges is shown.

The Yang-Lee zeros of the antiferromagnetic one-dimensional Blume-Capel model are studied in the same manner as the ferromagnetic ones. The dynamics of the location of the antiferromagnetic Yang-Lee zeros with respect to parameter $z=e^{J}$ is studied by finite size chain calculations and shown in the plots in Fig. 3. The distributions of the Yang-Lee zeros in the thermodynamic limit are in good agreement with the finite size chain calculations and are not shown in the plots in Fig. 3 in order to avoid overloading the plots with data. From the plots in Fig. 3 it follows that for high temperatures the Yang-Lee zeros lie on the negative part of the real axes only [Fig. 3(a)]. By decreasing the temperature the Yang-Lee zeros start to spread into the complex plane organizing circlelike structures as shown in Figs. 3(b)–3(f).

In Fig. 5(a) the Yang-Lee zeros are shown for different chain sizes N and in the thermodynamic limit ($N=10\,000$). From Fig. 5(a) it follows that the Yang-Lee zeros accumulate in the neighborhood of the edge singularity points. This is in good agreement with the thermodynamic limit calculations of the density of Yang-Lee zeros, which indicates a singular behavior of the density of Yang-Lee zeros at the edge singularity points (Fig. 2).

The details of finite size system symbolic and numerical calculation are given in Sec. VI of the paper.

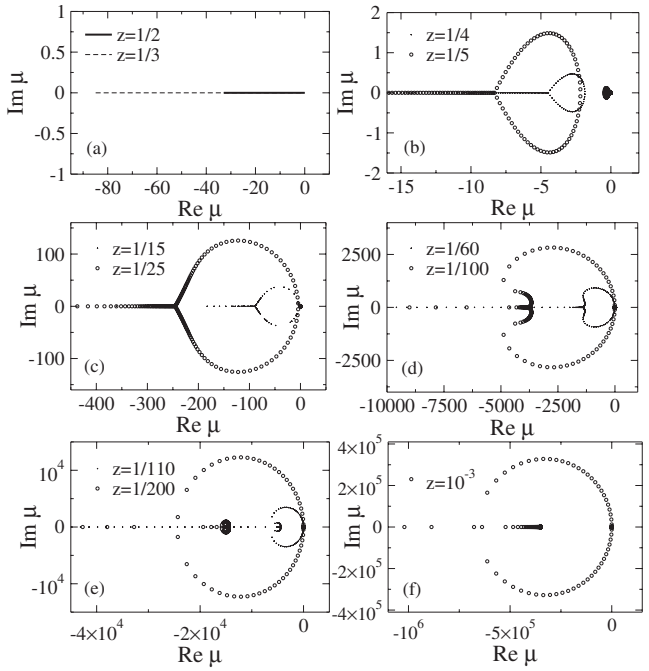

FIG. 3. The Yang-Lee zeros of the antiferromagnetic one-dimensional Blume-Capel model on complex $\mu=e^{h}$ plane for $y=e^{\Delta}=3$ and different values of $z=e^{J}$. The data are generated for finite size chains of $N=512$ spins. The real axes of the plots (b)–(f) are cut from below in order to show the nontrivial structure of the location of the Yang-Lee zeros. Note that the larger part of the data of the Yang-Lee zeros is located below the cutoff and lies over the negative real axes up to some negative value (not shown in the plots).

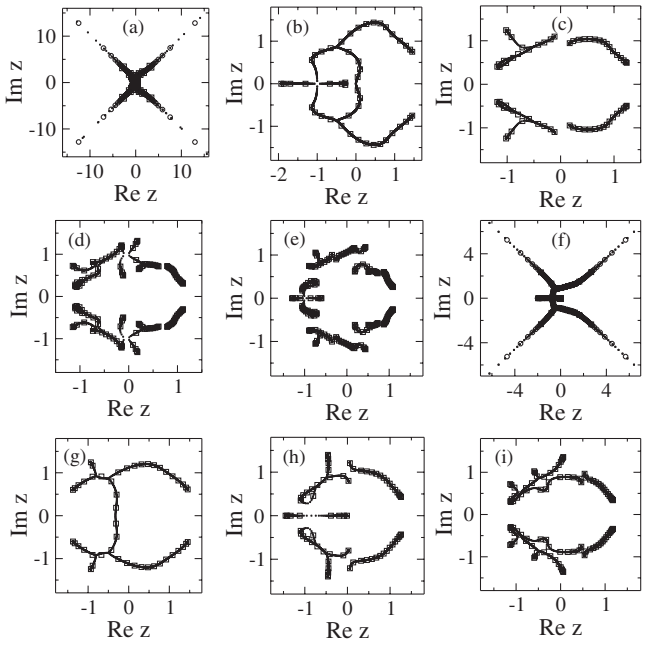

FIG. 4. The Fisher zeros of the one-dimensional Blume-Capel model on complex z plane for (a)–(e) $\bar{\Delta}=0$ and $\bar{h}=0,1,2,4,5$, respectively, and (f)–(i) $\bar{\Delta}=-1$ and $\bar{h}=0,1,2,3$, respectively. Small points represent the Fisher zeros in the thermodynamic limit for $N=10\,000$ spins. Boxes and circles correspond to finite size chain calculation data for $N=16$ and 1024 spins, respectively. Except for plots (a) and (f) the lines of Fisher zeros in the thermodynamic limit and $N=1024$ finite size system calculations are indistinguishable.

V. FISHER ZEROS

In this section the Fisher zeros of the one-dimensional BC model are investigated. By definition, the Fisher zeros correspond to zeros of the partition function with respect to a temperature dependent parameter. In general, the partition function of a BC model is a function of several parameters such as J, Δ, and h, which by the definition of Hamiltonian (1) are inversely proportional to temperature T. Formally, the parameters Δ and h may be considered proportional to J with some proportionality coefficients, i.e., $\Delta=\bar{\Delta}J$ and $h=\bar{h}J$. This procedure simply corresponds to renormalization of model parameters due to the freedom of choosing the units of energy measurement. After renormalization the partition function may be presented as a function of temperature parameter $z=e^{J}$, where parameters $y=e^{\Delta}$ and $\mu=e^{h}$ are replaced by $y=z^{\bar{\Delta}}$ and $\mu=z^{\bar{h}}$, respectively. In terms of z the transfer matrix can be written in the form

$$V=\begin{pmatrix} z^{1-\bar{\Delta}-\bar{h}} & z^{-(\bar{\Delta}+\bar{h})/2} & z^{-(\bar{\Delta}+1)} \\ z^{-(\bar{\Delta}+\bar{h})/2} & 1 & z^{-(\bar{\Delta}-\bar{h})/2} \\ z^{-(\bar{\Delta}+1)} & z^{-(\bar{\Delta}-\bar{h})/2} & z^{1-\bar{\Delta}+\bar{h}} \end{pmatrix}, \tag{26}$$

and Eq. (15) for the Fisher zeros becomes

$$F(\bar{h},\bar{\Delta},z,\varphi) \equiv (1+2\cos\varphi)^3\bar{a}_0^2 + 4\cos^2\tfrac{\varphi}{2}(\bar{a}_1^3+\bar{a}_0\bar{a}_2^3) - \bar{a}_1^2\bar{a}_2^2 - 2(1+2\cos\varphi)(2+\cos\varphi)\bar{a}_0\bar{a}_1\bar{a}_2 = 0, \tag{27}$$

where

$$\bar{a}_2 = 1 + z^{1-\bar{\Delta}}(z^{\bar{h}}+z^{-\bar{h}}),$$

$$\bar{a}_1 = z^{-\bar{\Delta}}(z^{\bar{h}}+z^{-\bar{h}})(z-1) + z^{-2\bar{\Delta}}(z^2-z^{-2}),$$

$$\bar{a}_0 = z^{-2\bar{\Delta}}(z^2-1)(1-z^{-1})^2.$$

In general, parameters $\bar{\Delta},\bar{h}$ may be considered as renormalized fields of the BC model.

Equation (27) can be solved numerically with respect to z to find the location of the Fisher zeros on the complex z plane. Note that only solutions to Eq. (27) satisfying condition (7) correspond to the Fisher zeros.

For simplicity let $\bar{h}$ and $\bar{\Delta}$ be integers. In this case Eq. (27) becomes a polynomial and the Fisher zeros may be found as zeros of this polynomial (see Fig. 4). The corresponding polynomial equation may be solved numerically [27]. If $\bar{h}$ and $\bar{\Delta}$ are rational numbers it is obvious that in that case Eq. (27) may be presented as a polynomial too. For irrational values of the $\bar{h}$ or $\bar{\Delta}$ Eq. (27) becomes a transcendental equation which in general is hard to solve. From the number theory it is well known that any irrational number

may be approximated by a rational number with arbitrary accuracy. Since Eq. (27) is an analytic function then irrational $\bar{h}$ and/or $\bar{\Delta}$ may be approximated by rational numbers and the solution to the corresponding equation will give a good approximation to the solution of the original equation. Thus using the procedure described above, the Fisher zeros may be calculated numerically within some predefined accuracy for any values of model parameters. Examples of the distributions of the Fisher zeros are given in Fig. 4. One can see that the Fisher zeros show a variety of different shapes (Fig. 4). On the other hand, from Fig. 4 it follows that the Fisher zeros are located on the lines ending at the Fisher edges. As for the Yang-Lee zeros, the condition $\varphi=0$ here also defines the Fisher edges.

In the case of integer or rational $\bar{h}$ and $\bar{\Delta}$ the order of the polynomial (27) with respect to z defines the number of Fisher edge singularity points. In general, the larger by modulus the values of $\bar{h}$ or $\bar{\Delta}$ the higher the order of polynomial (27). Thus the number of Fisher edges will be larger. On the other hand, the increase in the number of Fisher edges indicates that the number of connected components (curves) over which the Fisher zeros are distributed increases. For large values of $\bar{h}$ or $\bar{\Delta}$ this may lead to fractal-like structures for the distribution of the Fisher zeros. Hence the Fisher zeros are very sensitive to the values of parameters of the Hamiltonian which define the number of Fisher edges and thus significantly influence the topology of the distribution of the Fisher zeros.

The advantage of the method presented in this paper for studying the Fisher zeros is that it gives a mechanism for understanding the reason of sensitivity of the Fisher zeros on the model parameters as was mentioned in the Introduction.

Following the same procedure as for the density of the Yang-Lee zeros, a singular behavior for the density of Fisher zeros may be proved. For the Fisher zeros close to the Fisher edges, Taylor expansion of Eq. (27) with respect to φ in the vicinity of the edge point z_e $(\varphi=0)$ gives

$$z_i(\varphi) \approx z_e + \frac{\partial^2 z_i}{\partial^2 \varphi}\varphi^2 + o(\varphi^4), \tag{28}$$

with zero linear term in φ since $F(\bar{h},\bar{\Delta},z,\varphi)$ is an even function of φ. Using the same procedure as for the Yang-Lee edges, after simple algebra, for the density of Fisher zeros we get

$$g_f(\theta) \propto |\theta-\theta_e|^{-1/2}, \tag{29}$$

where θ_e and θ are phases of complex z temperatures at the Fisher edges and nearby points, respectively. Thus at all the Fisher edges the density of Fisher zeros has singular nature and the critical exponent $\sigma=-\frac{1}{2}$ is universal, i.e., σ does not depend on the model parameters.

Finite size system enumeration calculation over all microstates and finite size system symbolic and numerical calculations are performed for calculating the Fisher zeros of the one-dimensional BC model for chains up to $N=1024$ spins. The distributions of the Fisher zeros are in good agreement with the corresponding distributions in the thermodynamical limit. Examples of distributions of the Fisher zeros for different values of parameters are given in Fig. 4. The distribution of the Fisher zeros for different chain sizes N is given in Fig. 5(b). From Fig. 5(b) it follows that zeros of the partition function are distributed on several lines not lying on the unit circle and accumulate close to the edge singularity points. This is in good agreement with the thermodynamic limit calculations of the density of Fisher zeros indicating a singular behavior of the density of Fisher zeros at the edge singularity points.

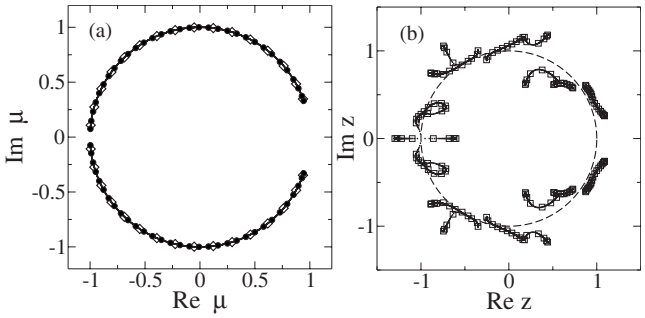

FIG. 5. Comparative plots of the partition function zeros for different finite size lattices and the thermodynamic limit. Continuous lines correspond to the partition function zeros in the thermodynamic limit. (a) The Yang-Lee zeros for $y=3$, $z=4$ and chain sizes $N=16$ (diamonds) and $N=32$ (bold points). (b) The Fisher zeros for $\bar{\Delta}=0$, $\bar{h}=5$ and chain size $N=16$ (boxes). The unit circle is shown as a dashed curve.

VI. DISCUSSION OF NUMERICAL METHODS

To confirm the results of calculations in the thermodynamic limit presented in Secs. IV and V of the paper several numerical tests were performed on finite size systems. First, we performed exact finite size enumeration calculations over all microstates of the one-dimensional BC model for up to $N=22$ spins. The exact finite size enumeration method is quite simple and may be easily generalized to one or high dimensional lattice spin-S Ising-type models. It is based on the idea of mapping the spin-S model of the total number of spins N on any lattice into an N-digit number in base-S presentation. For simplicity the algorithm is presented here for the one-dimensional BC model of N spins $s_i=-1,0,1$, and $i=1,\ldots,N$.

Consider the chain of N spins of the BC model as an N-digit number in ternary (base-3) presentation, i.e., map the spin configuration $\{s_N,\ldots,s_2,s_1\}$ into N-digit number $\sigma_N\cdots\sigma_2\sigma_{13}$, where $\sigma_i=s_i+1$ and σ_i takes values 0, 1, 2. In terms of numbers the spin configuration $\{-1,\ldots,-1,-1\}$ corresponds to zero and the configuration $\{1,\ldots,1,1\}$ corresponds to the maximal N-digit number in ternary presentation $\overline{2\cdots22}_3$. All numbers from 0 to $\overline{2\cdots22}_3$ may be generated in a finite number of steps by adding $1\equiv\overline{0\cdots01}_3$ to 0. Thus using the inverse transformation from numbers to spin configurations $s_i=\sigma_i-1$ all spin configurations of the model may be generated. For any spin configuration generated in this way the energy of the configuration may be calculated using Eq. (1) and the finite size partition function (2)

is constructed. Any time a new configuration is generated the total energy of the system Eq. (1) is calculated. This is due to the fact that the new configuration that was sampled is not always generated from the previous one by a single spin flip. For example, two spins should be flipped in order to pass from the spin configuration $\{-1,\ldots,-1,-1,1\}$ to the configuration $\{-1,\ldots,-1,0,-1\}$ which in terms of ternary arithmetic corresponds to the following relation: $\overline{0\cdots02}_3+1_3=\overline{0\cdots10}_3$. The computational speed of the algorithm may be improved if all configurations of the system may be generated consequently by a single spin flip. In that case the energy of the system may be updated by adding to the energy of the previous configuration the energy change between the neighbor interactive spins for the flipped spin due to the nearest neighbor interaction nature of the BC model Hamiltonian, Eq. (1). To the best knowledge of the authors no simple modification of this algorithm is known that will take into account the advantage of single spin flip passage in generating new configurations. On the other hand, the total number of configurations of the spin-S Ising-type model of N spins is S^N. For the case of the one-dimensional Blume-Capel model with $N=22$ spins this leads to $3^{22}\approx 3\times 10^{10}$ configurations. Numerical tests showed that for the one-dimensional BC model, zeros of the partition function of finite size systems start to converge to the ones in the thermodynamic limit started from $N=16$ system sizes (Fig. 5). It took about 72 h on a Pentium IV 1.81 GHz computer to calculate the partition function for $N=22$ spins with this method. Increasing the number of spins exponentially increases the number of configurations and the run time of the program. Thus with the exact enumeration method of all configurations the maximal size of the system was considered to be $N=22$. In conclusion to this description we note that the algorithm presented here is quite easy to adopt for constructing the partition functions for getting both the Yang-Lee and the Fisher zeros. The generalization of the algorithm to other Ising-type models is quite straightforward and it is not presented here.

As it was indicated above, the method of exact enumeration of all possible states of the BC model does not allow us to study finite size systems with a large number of spins. Since it is a one-dimensional model and we are interested in considering as large systems as possible. Hence another method for generating the partition function polynomial was used.

The method uses the transfer matrix method and symbolic computation software like MATHEMATICA for constructing the partition function polynomial as given by Eq. (4). In order to avoid operations with rational expressions it is convenient to define the transfer matrix in the way that powers of variables μ and z for the Yang-Lee and Fisher zeros, respectively, are positive for all elements of the transfer matrix. For example, for studying the Yang-Lee zeros of the BC model with $J>0$, $\Delta<0$ it is convenient to define the transfer matrix as follows:

$$V(s_i,s_{i+1})=\exp[J(1+s_is_{i+1})-\Delta s_i^2+h(1+s_i)],$$

and

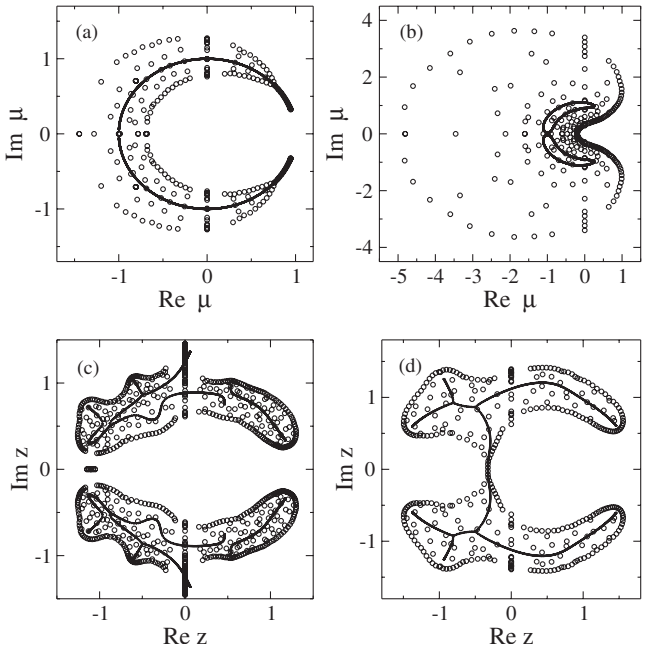

FIG. 6. Examples of numerical instabilities in the distribution of the Yang-Lee zeros for $y=3$ and (a) $z=4$, (b) $z=2$, and the Fisher zeros for $\bar{\Delta}=-1$ and (c) $\bar{h}=3$, (d) $\bar{h}=1$ of finite size chain BC model. Circles and solid lines correspond to solutions to the partition function polynomial for finite size system with MATHEMATICA ($N=128$) and MPSOLVE ($N=1024$), respectively.

$$V=\begin{pmatrix} tz^2 & tz & t \\ z\mu & z\mu & z\mu \\ t\mu^2 & tz\mu^2 & tz^2\mu^2 \end{pmatrix}, \tag{30}$$

where $\mu=e^h$, $z=e^J$, and $t=1/y=e^{-\Delta}$. Since the Hamiltonian is defined within any arbitrary constant, the transfer matrix (30) is equivalent to the one used in Sec. II. By setting the values of parameters z and t and using symbolic computation software such as MATHEMATICA the polynomial equation for the Yang-Lee zeros may be generated from the equation

$$Z_N=\mathrm{Tr}V^N=0, \tag{31}$$

and the coefficients of the polynomial written to the file in a format suitable for the MPSOLVE program [27]. In this paper the MPSOLVE program was used for solving high order polynomial equations because the algorithm used in this program gives the most stable results. It is interesting to note that solutions to polynomial Eq. (31) show instability at the complex plane when coefficients of the polynomial are floating point (decimal) numbers as shown in Fig. 6. To overcome this difficulty we converted the values of parameters z and t into rational fractions and used a special input format of the MPSOLVE program to solve polynomial equations with rational coefficients. In this case the numerical instability in solutions disappears and we get excellent agreement with thermodynamic limit data even for $N=1024$ spins (with the corresponding polynomial equation of order 2048 for the Yang-Lee zeros). We could not find such an option in MATHEMATICA which demonstrates divergence of the Yang-

Lee zeros data from the thermodynamic limit values for system sizes $N>32$ spins. It should be noted that the MPSOLVE program also demonstrates such an instability when coefficients of the polynomial are floating point numbers with some predefined accuracy, but passing to rational form for coefficients of the polynomial equation fixes the problem.

Finite size system calculations of the Fisher zeros may be performed in the same manner as given above. Note that for the Fisher zeros the coefficients of the polynomial equation are integers. This directly follows from the definition of the transfer matrix given in Eq. (26) where for all the elements of the transfer matrix coefficients of z terms are equal to 1. For this case it is convenient to use the option of the MPSOLVE program for solving polynomial equations with integer coefficients which leads to stable solutions even for $N=1024$ spins for different values of $\bar{h}$ and $\bar{\Delta}$. Using this method an excellent agreement with the thermodynamic limit data is obtained (Fig. 4).

The run time of the MPSOLVE program for the examples considered in this paper was from several seconds up to several hours for $N=32$ and $N=1024$, respectively.

By performing a number of simulations we conclude that zeros of the partition function are sensitive to the accuracy of coefficients of the corresponding polynomial equation and passing to the rational or integer form of presentation of the polynomial coefficients gives stable results and correct location of zeros of the partition function when using the MPSOLVE program [27].

VII. CONCLUSION

We have used the transfer matrix method to study the partition function zeros of the one-dimensional Blume-Capel model. A method for finding the partition function zeros is described. The distributions of the Yang-Lee and Fisher zeros for different values of parameters of the model are found. The ferromagnetic and antiferromagnetic Yang-Lee zeros are investigated. The resulting distributions of the ferromagnetic Yang-Lee zeros are in good agreement with results given in [14,17]. The distribution of the Fisher zeros gives a variety of shapes, different from the unit circle. The triple degeneracy case is discussed and no partition function zeros are found in that case.

Exact finite size enumeration and finite size system symbolic computational methods are used to compute the Yang-Lee and Fisher zeros for up to $N=1024$ spins. Resulting distributions of zeros are consistent with the corresponding distributions in the thermodynamic limit.

Locations of the Yang-Lee and Fisher edge singularity points are found from the condition $\varphi=0$. Also, we have described the behavior of the densities of the partition function zeros at the edge singularity points and found corresponding critical exponents. To the best knowledge of the authors the Fisher zeros and the corresponding edge singularity exponents for the one-dimensional Blume-Capel model are calculated in the present work for the first time. The critical exponents for both the Yang-Lee and Fisher edge singularities are found to be the same and equal to $\sigma=-\frac{1}{2}$. This equivalence indicates the universality of edge singularity exponents for one-dimensional models. The same values for the edge singularity exponents are found for the one-dimensional Ising and Potts models also [6].

ACKNOWLEDGMENTS

The authors are grateful to L. N. Ananikyan for useful discussions. This work was partly supported by Grant No. ANSEF PS-condmatth-521.

[1] C. N. Yang and T. D. Lee, Phys. Rev. **87**, 404 (1952); T. D. Lee and C. N. Yang, *ibid.* **87**, 410 (1952).
[2] M. E. Fisher, in *Lectures in Theoretical Physics*, edited by W. E. Brittin (University of Colorado Press, Boulder, CO, 1965), Vol. 7C, p. 1.
[3] I. Bena, M. Droz, and A. Lipowski, Int. J. Mod. Phys. B **19**, 4269 (2005).
[4] R. G. Ghulghazaryan, N. S. Ananikian, and P. M. A. Sloot, Phys. Rev. E **66**, 046110 (2002); N. S. Ananikian and R. G. Ghulghazaryan, J. Comput. Methods Sci. Eng. **2**, 75 (2002); S.-Y. Kim, Phys. Rev. E **74**, 011119 (2006); **71**, 017102 (2005).
[5] M. Biskup, C. Borgs, J. T. Chayes, L. J. Kleinwaks, and R. Kotecký, Phys. Rev. Lett. **84**, 4794 (2000).
[6] R. G. Ghulghazaryan and N. S. Ananikian, J. Phys. A **36**, 6297 (2003); S.-Y. Kim, J. Korean Phys. Soc. **44**, 495 (2004); Z. Glumac and K. Uzelac, J. Phys. A **24**, 501 (1991).
[7] D. Ruelle, Phys. Rev. Lett. **26**, 303 (1971); C. M. Newman, J. Stat. Phys. **15**, 399 (1976); E. H. Lieb and A. D. Sokal, Commun. Math. Phys. **80**, 153 (1981).
[8] C. M. Newman, Commun. Math. Phys. **41**, 1 (1975); A. D. Sokal, J. Stat. Phys. **25**, 25 (1981).
[9] P. J. Kortman and R. B. Griffiths, Phys. Rev. Lett. **27**, 1439 (1971); M. E. Fisher, *ibid.* **40**, 1610 (1978).
[10] W. Janke, D. A. Johnston, and R. Kenna, Nucl. Phys. B **682**, 618 (2004); M. Suzuki, J. Math. Phys. **9**, 2064 (1968); R. Abe, Prog. Theor. Phys. **38**, 586 (1967); Y. Park and M. E. Fisher, Phys. Rev. E **60**, 6323 (1999).
[11] V. Matveev and R. S. Shrock, Phys. Rev. E **53**, 254 (1996); W. T. Lu and F. Y. Wu, J. Stat. Phys. **102**, 953 (2001); M. L. Glasser, V. Privman, and L. S. Schulman, Phys. Rev. B **35**, 1841 (1987); J. Stephenson, J. Phys. A **20**, 4513 (1987).
[12] P. Tong and X. Liu, Phys. Rev. Lett. **97**, 017201 (2006); J. L. Jacobsen and J. Salas, J. Stat. Phys. **122**, 705 (2006); Sh.-Ch. Chang and R. Shrock, J. Phys. Math. Gen. **39**, 10277 (2006).
[13] M. E. Fisher, Suppl. Prog. Theor. Phys. **69**, 14 (1980).
[14] X.-Z. Wang and J. S. Kim, Phys. Rev. E **58**, 4174 (1998).
[15] D. A. Kurtze, J. Stat. Phys. **30**, 15 (1983); W. van Saarloos and D. A. Kurtze, J. Phys. A **17**, 1301 (1984).
[16] S. Katsura and M. Ohminami, J. Phys. A **5**, 95 (1972).
[17] L. A. F. Almeida and D. Dalmazi, J. Phys. A **38**, 6863 (2005).
[18] M. Blume, Phys. Rev. **141**, 517 (1966); H. W. Capel, Physica

(Amsterdam) **32**, 966 (1966).
[19] M. Blume, V. J. Emery, and R. B. Griffiths, Phys. Rev. A **4**, 1071 (1971).
[20] E. R. Dobbs, *Helium Three* (Oxford University Press, Oxford, UK, 2002); C. La Pair *et al.*, Physica (Amsterdam) **29**, 755 (1963).
[21] A. Blatter and M. von Allmen, Phys. Rev. Lett. **54**, 2103 (1985); W. Sinkler, C. Michaelsen, R. Bormann, D. Spilsbury, and N. Cowlam, Phys. Rev. B **55**, 2874 (1997).
[22] G. P. Johari, Physiol. Chem. Phys. **3**, 2483 (2001); P. E. Cladis, R. K. Bogardus, W. B. Daniels, and G. N. Taylor, Phys. Rev. Lett. **39**, 720 (1977).
[23] O. Mishima and H. E. Stanley, Nature (London) **396**, 329 (1998).
[24] D. Ertas and D. R. Nelson, Physica C **272**, 79 (1996); N. Avraham *et al.*, Nature (London) **411**, 451 (2001).
[25] J. Zhang, X. Peng, A. Jonas, and J. Jonas, Biochemistry **34**, 8631 (1995); M. I. Marqués, J. M. Borreguero, H. E. Stanley, and N. V. Dokholyan, Phys. Rev. Lett. **91**, 138103 (2003).
[26] S. Rastogi, G. W. H. Hohne, and A. Keller, Macromolecules **32**, 8897 (1999); A. L. Greer, Nature (London) **404**, 134 (2000).
[27] MPSolve 2.2 multiprecision polynomial solver by D. A. Bini was used for solving polynomial equations (http://fibonacci.dm.unipi.it/~bini/ric.html).